TITLE

IL-12 and IL-15 induce the expression of CXCR6 and CD49a on peripheral natural killer cells

AUTHORS

Theresa Hydes[1], Angela Noll[2], Gabriela Salinas-Riester[3], Mohammed Abuhilal[4], Thomas Armstrong[4], Zaed Hamady[4], John Primrose[4], Arjun Takhar, Lutz Walter[2], Salim I Khakoo[1]

[1] Clinical and Experimental Sciences, Faculty of Medicine, University of Southampton, Southampton, UK

[2] Primate Genetics Laboratory, German Primate Centre, Göttingen, Germany

[3] Transcriptome and Genome Analysis Laboratory Göttingen, University Medical Centre Göttingen, Germany

[4] Hepatobiliary Surgery, University Hospital Southampton NHS Foundation Trust, Southampton, UK

KEY WORDS

Natural Killer Cells
CD49a antigen
Chemokine Receptor 6 Protein, human
Liver
Cytokines

CORRESPONDING AUTHOR

Salim Khakoo
Faculty of Medicine
University of Southampton
Mailpoint 811
Level E South Academic Block
Southampton General Hospital
Tremona Road
Southampton
SO16 6YD
Tel: 023 8079 6671/5099
Fax: 023 8051 1761
E-mail: s.i.khakoo@soton.ac.uk

ABBREVIATIONS

B3GAT1	Galactosylgalactosylxylosylprotein 3-beta-glucuronosyltransferase 1
CCL	CC chemokine ligand
CCR	CC chemokine receptor
CCRL	CC chemokine receptor-like
CD	Cluster of Differentiation
CFSE	Carboxyfluorecin succinimidyl ester
CMV	Cytomegalovirus
CRTAM	Class-I MHC-restricted T-cell associated molecule
CXCR	Chemokine receptor
Eomes	Eomesodermin
FCGR3AFc	Fragment Of IgG Receptor IIIa
FLNA	Filamin
GNLY	Granulysin
HLA	Human leukocyte antigen
ICAM	Intercellular Adhesion Molecule
IFNγ	Interferon gamma
IL	Interleukin
KIR	Killer cell immunoglobulin-like receptor
NK	Natural killer
NKIB	Natural killer cell isolation buffer
PXN	Paxillin
RNA	Ribonucleic acid
S1PR1	Sphingosine-1-phosphate receptor 1
TIGIT	T-Cell Immunoreceptor With Ig And ITIM Domains
TNFα	Tissue necrosis factor alpha
TRAIL	Tissue necrosis factor-related apoptosis-inducing ligand

ABSTRACT

Murine hepatic NK cells exhibit adaptive features, with liver-specific adhesion molecules CXCR6 and CD49a acting as surface markers. We investigated human liver-resident CXCR6+ and CD49a+ NK cells using RNA sequencing, flow cytometry and functional analysis. We further assessed the role of cytokines in generating NK cells with these phenotypes from the peripheral blood. Hepatic CD49a+ NK cells could be induced using cytokines and produce high quantities of IFNγ and TNFα, in contrast to hepatic CXCR6+ NK cells. RNA sequencing of liver-resident CXCR6+ NK cells confirmed a tolerant immature phenotype with reduced expression of markers associated with maturity and cytotoxicity. Liver-resident double-positive CXCR6+CD49a+ hepatic NK cells are immature but maintain high expression of Th1 cytokines as observed for single-positive CD49a+ NK cells. We show that stimulation with activating cytokines can readily induce upregulation of both CD49a and CXCR6 on NK cells in the peripheral blood. In particular IL-12 and IL-15 can generate CXCR6+CD49a+ NK cells in vitro from NK cells isolated from the peripheral blood, with comparable phenotypic and functional features to liver-resident CD49a+ NK cells, including enhanced IFNγ and NKG2C expression. IL-12 and IL-15 may be key for generating NK cells with a tissue-homing phenotype and strong Th1 cytokine profile in the blood, and links peripheral activation of NK cells with tissue-homing. These findings may have important therapeutic implications for immunotherapy of chronic liver disease.

INTRODUCTION

Natural Killer (NK) cells provide first line defence against virally-infected and cancer cells. They comprise nearly 50% of the hepatic lymphocyte population [1,2] and play a role in the pathogenesis of several liver diseases. Polymorphisms within the NK cell Killer-cell Immunoglobulin-like Receptors (KIR) and their Human leukocyte antigen (HLA) ligands are known to influence outcomes for Hepatitis B and C viral infections and susceptibility towards hepatocellular carcinoma.[3–7] Skewed NK cell phenotypes can also influence disease progression. In hepatitis C, enrichment of Nkp46+ NK cells in the liver and hypofuctional4 CD56-CD16+ NK cells in the blood, are associated with poor treatment responses.[8,9] Furthermore NK cell cytotoxicity, cytokine release and tumour surveillance are impaired in pre-cancerous fibrosis and cirrhosis and tumour-infiltrating regions of the liver.[10] The induction of ‘hyperfunctional’ NK cell phenotypes in the liver may therefore improve outcomes in liver diseases.

While NK cells are classically members of the innate immune system, selected populations in mice and macaques display antigen-specific memory towards haptens [11–13] and viral antigens.[11,14–16] The chemokine receptor (CXCR), CXCR6 [12] and adhesion molecule CD49a [13] have been identified as surface markers of memory NK cells in mice. Interestingly these features were generally limited to liver-resident NK cells. NK subsets expressing both CD49a [17] and CXCR6 [18–20] have since been identified in the human liver and are generally absent from peripheral blood. CD49a+ NK cells have been described as T-bet+Eomes-. The majority are NKG2C+ with an oligoclonal KIR expression pattern consistent with having undergone clonal expansion. They also have strong proliferative capabilities and have therefore been described as having adaptive features. Liver-resident CD49a+ NK cells highly express Th1 cytokines, but show poor degranulation.[17] Conversely CXCR6+ NK cells are T-bet^{low}Eomes^{high} with poor production of inflammatory cytokines and cytotoxic mediators.[20] CXCR6+ NK cells are a major liver-resident NK cell population, comprising nearly 60% of hepatic NK cells.[20] They express CCR5 and may play a role in liver-homing through their interaction with CCL3, CCL5 and CXCL16.[18] CXCR6+ NK cells appear to be immunotolerant, with reduced production of interferon gamma (IFNγ), tumour necrosis factor alpha (TNFα), perforin and granyme B.[20] CXCR6+CD69+ NK cells have also recently been described in human lymphoid tissue and therefore CXCR6 is likely to be a marker of general tissue-residency.[21] In summary, liver-resident CD49a+ and CXCR6+ NK subsets appear distinct. There has been no direct comparison of these two subsets within the same cohort.

While antigen-specific memory has not been demonstrated in human NK cells, many studies have shown that they possess adaptive features. Clonal expansion of NKG2C+ NK cells in the peripheral blood has been seen following viral infection, particularly cytomegalovirus infection (CMV).[22–24] Furthermore NK cells in mice and humans display adaptive behaviour in response to a combination of pro-inflammatory cytokines, interleukin (IL)-12, IL-15 and IL-18.[25–27] Cytokines 'prime' NK cells resulting in enhanced interferon gamma (IFNγ) release on re-stimulation, enhanced proliferation [25,26] and longevity.[25]

The unique hepatic cytokine microenvironment may drive NK cell differentiation towards functionally distinct liver-resident subsets.[28,29] This may promote tolerance in health in the face of large volumes of non-self antigens from the portal vein, and an activated 'hyperfunctional' phenotype during disease. It is therefore important to understand how NK cells expressing tissue-resident markers CXCR6+ and CD49a+ are influenced by cytokines as this may impact liver disease. Cytokine-induced memory-like NK cells have already demonstrated therapeutic benefit for haematological malignancies [27,30] and the accumulation of these in the liver may open doors for novel immunological therapies for viral hepatitis and liver cancer.

We therefore performed a direct phenotypic and functional comparison of liver-resident CXCR6+ and CD49a+ NK cells in humans and assessed the role of cytokines in generating NK cells with this phenotype in both the liver and peripheral blood.

RESULTS

CD49a+ NK cells are found in a small percentage of the population, whereas CXCR6+ cells are found universally

Liver mononuclear cells were isolated from the unaffected liver margin of 52 patients who had undergone hepatic resection, with paired peripheral blood samples obtained for 29 individuals. We observed CXCR6+ NK cells in all individuals with a median frequency of 57.7% (range 17.4 – 91.1%), whereas CD49a+ NK cell frequencies were lower, median frequency 7.8% (range 2.3 – 69.0%) (**Figure 1a,b**). Both subsets were virtually absent from the peripheral blood; 4.0% (range 0.5 – 29.5%) and 1.9% (range 0.3 – 12.0%) respectively (**Figure 1a,b**). Only 3/35 individuals (8.6%) had high frequencies of hepatic CD49a+ NK cells (>30% of the overall NK cell population) (**Figure 1c**), compared to 31/34 (91.%) for CXCR6+ NK cells. Thus CXCR6+ NK cells represent the dominant liver-specific NK cell sub-population. Only 3.9% of hepatic NK cells were CD49a+CXCR6+ ʹdouble-positive’ (range 1.5 – 25.7%) with a third of individuals (8/27) displaying much higher frequencies (6.3 – 25.7%), dictated by CD49a expression (**Figure 1c**). The majority of NK cells in the human liver were CXCR6+CD49a- (42.1%) or CXCR6-CD49a- (31.8%) (**Figure 1d**). Importantly frequencies of CXCR6+ and CD49a+ NK cells were similar whether perfusion or tissue digestion isolation techniques were used **(Supplementary Figure 1**).

CD49a+ and CXCR6+ hepatic NK cells are phenotypically distinct

Both CD49a and CXCR6 are markers of adaptive NK cells in mice, therefore to determine whether CD49a+ and CXCR6+ NK cells might represent adaptive NK cells in humans, we began by comparing their expression of markers of maturity and function. Separation of hepatic NK cell into CD49a+CXCR6+, CD49a+CXCR6-, CD49a-CXCR6+ and CD49a-CXCR6- subsets demonstrated CXCR6 expression was associated with low levels of CD16 and CD57 and high levels of CD69 (**Figure 1e**). Conversely CD49a+ NK cells were more likely to be NKG2C+ or KIR+ compared to CD49a- NK cells. Therefore, CD49a+CXCR6+ NK cells were CD69+CD16^{low}CD57^{low} with a higher frequency of KIR and NKG2C expression compared to CD49a- NK cells (**Figure 1e**).

CD49a+ and CXCR6+ hepatic NK cells are functionally distinct

Following stimulation with IL-12 and IL-15 hepatic NK cells expressing CD49a produced greater quantities of IFNγ (7.5% vs 1.6%, $p<0.05$) and tumour necrosis factor alpha (TNFα) (22.5 vs 2.4%, $p<0.05$) compared to CD49a- NK cells. On CD49a+ NK cells, IFNγ production remained high irrespective of CXCR6 expression, and TNFα expression was particularly high on CD49a+CXCR6+ NK cells (**Figure 1f**). Thus double-positive CD49a+CXCR6+ cells behave more like single-positive CD49a 'adaptive-like' NK cells, than single-positive CXCR6+ NK cells.

Transcriptomic analysis of CXCR6+ and CXCR6- liver-resident NK cells

As hepatic CXCR6+ NK cells are known to have a distinct transcriptional profile within the liver and do not appear to be 'adaptive', we performed RNA sequencing of paired sorted liver-resident CXCR6+ and CXCR6- NK cells from three individuals with colorectal metastases to better understand their role. Calculation of Euclidian distances revealed a close similarity among the three CXCR6-negative samples and three CXCR6-positive samples (**Figure 2a**). We used R package DESeq2 [31] to analyse the differential expression of genes between the two groups using a p-value adjusted for multiple comparisons according to Benjamini Hochberg **(Supplementary Table 2)**, and plotted the top 75 differentially expressed genes (**Figure 2b**). This analysis revealed reduced expression of genes associated with maturity and cytotoxicity in liver-resident CXCR6+ NK cells including KIR, CD16 (FCGR3A), CD57 (B3GAT1), granulysin (GNLY), granzyme B and H, and desmoyokin (AHNAK) (**Figure 2b**). The latter is found on mature cytotoxic T-cells and controls calcium signalling during cytolysis.[32] In addition lower transcript levels of nesprins, SYNE1 and SYNE2, were found in CXCR6+ NK cells. These code for proteins involved in tethering the centrosome to the nucleus, however this process has been shown to not affect cytotoxicity in T-cells.[33] CXCR6+ NK cells also displayed downregulation of signalling proteins promoting migration of lymphocytes out of tissue into the circulation (Sphingosine-1-phosphate receptor 1 (S1PR1), paxillin (PXN)) (**Figure 2b**).

Furthermore CXCR6+ NK cells expressed higher levels of Eomes and lower levels of T-bet (TBX21) compared to CXCR6- NK cells (**Figure 2c**).[20,29] In terms of tissue residency they were CD69+ CD49e- (**Figure 2c**).[18,20,34,35] CXCR6+ NK cells showed upregulation of CC chemokine receptor (CCR) 5 which may support their migration towards, and long-term residence in the liver (**Figure 2c**).[18,29] However expression of CXCR2 and CX3CR1 were reduced, which code for receptors thought to be responsible for the movement of CD56^{dim}

NK cells towards the liver as part of their free movement between compartments (**Figure 2b**).[18] In addition CXCR6+ NK cells displayed upregulation of adhesion molecules (ICAM1, PATJ) (**Figure 2c**). Of note we did not observe over-expression of CD2, recently identified to be critical for the adaptive behaviour of the NKG2C+CD57+ NK cells in hCMV.[36] Finally to determine the potential for CXCR6+ liver-resident NK cells to respond to cytokines used to generate memory-like NK cells in the blood, we studied signalling pathways for IL-2, IL-12, IL-15 and IL-18. We observed upregulation of the IL-23R gene, as recently described by Cuff et al [29], which pairs with IL-12RB1, although the latter was down-regulated; in addition to upregulation of IL-12RB2 and IL-2R (**Figure 2c**). There was no consistent significant differential expression of other receptors or downstream signalling molecules within these pathways.

Culture of hepatic MNCs with activating cytokines leads to an increase in CD49a+ NK cell frequencies, with no further enrichment of the CXCR6+ NK subset

Having identified both CXCR6+ and CD49a+ NK cells in the human liver, we investigated their response towards activating cytokines, particularly the cytokine cocktail used to induce memory-like NK cells in the peripheral blood. Following culture with IL-2, IL-12, IL-15, IL-18 or the cytokine cocktail (IL-2/IL-12/15/18) proliferating hepatic NK cells preferentially showed upregulation of CD49a rather than CXCR6 (**Figure 3a,b**). Expression of CD49a on NK cells increased from 8.7% at rest to 77.1% (IL-2), 55.7% (IL-12), 83.9% (IL-15), 85.7% (IL-18) and 88.9% (cytokine cocktail). Frequencies of hepatic CXCR6+ NK cells did not increase significantly beyond their resting levels under the same conditions, with a negligible change of CXCR6 on dividing NK cells from 65.1% at day 0 to 65.5%, 64.2% and 56.7% with IL-2, IL-15 and IL-18 (**Figure 3b**). IL-12 generated the highest number of CXCR6+ NK cells by day six (74.1%) (**Figure 3b**). Culture with the cytokine cocktail led to a decrease in the percentage of NK cells expressing CXCR6 (to 24.2% of total NK cells), in sharp contrast to its ability to upregulate CD49a (**Figure 3b**).

The generation of high frequencies of CD49a+ NK cells following culture with activating cytokines, resulted in a significant increase in the percentage of double-positive CD49a+CXCR6+ NK cells seen within the hepatic NK cell population in vitro (**Figure 3c**). This was true following culture with IL-2, IL-12, IL-15 and IL-18 individually, but not the cytokine cocktail as a result of its negative influence on the frequency of CXCR6+ NK cells (**Figure 3c**).

Therefore, in common with our functional data, liver-resident CD49a+ but not CXCR6+ NK cells appear to be reactive towards cytokines, particularly the cytokine cocktail.

The cytokine cocktail and IL-15 induced the strongest proliferation of hepatic NK cells (**Figure 3d**). CFSE MFI results suggested a superior proliferation of NK cells expressing CD49a over those expressing CXCR6 at day six, following culture with IL-15 or the cytokine cocktail. Differences between cytokines on NK cell proliferation as a whole were significantly greater than differences seen between NK cell subsets (**Figure 3d, Supplementary Figure 2**). It is however not possible to conclude whether enrichment of CD49a+ NK cells within the hepatic NK cell population occurs as a result of enhanced proliferation of existing CD49a+ NK cells, or due to de novo upregulation and on previously negative cells. Marquardt et al previously sorted these populations prior to culture with IL-15 and feeder cells and reported an 800 fold expansion of CD49a+ NK cells over three weeks, but also upregulation of CD49a on CD49a- NK cells suggesting that both mechanisms may operate.

CD49a and CXCR6 expression can be induced on peripheral blood NK cells in vitro

Despite resting populations in the peripheral blood being small, cytokines were able to induce a large increase in CD49a+ NK cells frequencies from 2.1% (0.7% to 4.3%) to 98% (90.6% - 99.9%), cytokine cocktail; 83.3% (27.7% - 98.3%), IL-18; 71.9% (33.9% - 88.3%), IL-15; 71.3% (13.1% - 95.7%), IL-12 and 66.9% (11.3% - 95.6%), IL-2 (**Figure 4a, b**), accompanied by an increase in absolute numbers of CD49a+ NK cells (**Figure 4c**). In contrast to the liver CXCR6 could be up-regulated on peripheral blood NK cells, with an increase in median frequency of CXCR6+ NK cells from 3.1% (1.5% - 14.6%) to 10.9% (2.8% – 54.2%), IL-2; 21.4% (5.6% - 59.9%), IL-12 and 23.3% (3.5% - 60.5%), IL-15 (**Figure 4b**). Frequencies remained unchanged with IL-18 (4.1%, 1.5% to 48.4%) and the cytokine cocktail (5.6%, 2.1% to 76.1%), although there was a large degree of individual variability. As frequencies of CXCR6+ NK cells were lower at day six compared to CD49a+ NK cells, a significant increase in the total number of CXCR6+ NK cells in vitro could only be observed following culture with IL-15 (associated with the highest viability of NK cells overall) (**Figure 4c**). Importantly IL-15 (15.7%) and IL-12 (10.8%) were the most effective cytokines at inducing CD49a+CXCR6+ double-positive NK cells compared to IL-2 (5.5%), IL-18 (3.1%) and the cytokine cocktail (4.5%) following six days of culture (**Figure 4d**). In common with liver, IL-15 and the cytokine cocktail supported the greatest proliferation of NK cells (**Figure 4e**).

In order to examine the influence of specific cytokines on the induction of CXCR6+ and CD49a+ NK cells we cultured purified NK cells isolated from the peripheral blood in IL-12 and IL-15 for 12 hours. CD49a+ NK cells could be induced using both IL-12 (4.1%) and IL-15 (9.0%), whereas CXCR6+ NK cells could only be induced at this time point using IL-12, from a resting frequency of 2.1% to 4.0% (12 hours of IL-15, frequency 2.1%) (**Figure 4f**).

Cytokine-induced peripheral blood CD49a+CXCR6+ NK cells are CD56^{bright}CD69+ with a higher frequency of NKG2C+ NK cells compared to other NK subsets

Cytokine-induced CD49a+ NK cells generated in vitro displayed a similar phenotype to liver-resident CD49a+ NK cells, being CD56^{bright} (68.8%) and CD69+ (83.0%) following IL-15 stimulation. While peripheral blood CD49a- NK cells also highly expressed both markers under these conditions, CD49a+ populations contained a greater frequency of NKG2C+ NK cells than populations that remained CD49a- (37.7% vs 19.6%, $p<0.01$) (**Supplementary Figure 3**) and CD49a+ liver-resident NK cells (37.7% vs 10.3%, $p<0.05$). The majority of cytokine-induced CXCR6+ NK cells generated in the peripheral blood were CD56^{bright} (73.3%) CD69+ (81.4%) (**Supplementary Figure 3**), indicative that they display similar levels of markers of maturation and liver-residency as those found in the liver tissue. However cytokine-induced CXCR6+ NK cells contained higher frequencies of NKG2C+ NK cells compared to peripheral NK cells that remained CXCR6- in the presence of IL-15 (47.5% vs 25.0%, $p<0.01$), and resting liver-resident CXCR6+ NK cells (47.5% vs 5.9%, $p<0.0001$) (**Supplementary Figure 3**). Significant differences were also seen for CD49a expression compared to peripheral NK cells that remain CXCR6- (83.0% vs 63.0%, $p<0.01$) and liver-resident CXCR6+ NK cells (83.0% vs 8.9%, $p<0.0001$) (**Supplementary Figure 3**).

Frequencies of double-positive CD49a+CXCR6+ NK cells were therefore higher following six days of cytokine stimulation of peripheral blood NK cells, than found in situ in the liver (3.9% vs 15.7%, $p<0.05$ (IL-15)) (**Figure 1d, Figure 4c**). A direct comparison of the phenotype of resting liver-resident CD49a+CXCR6+ NK cells and those generated through IL-15 stimulation in the peripheral blood demonstrated high levels of CD69 (83.4% vs 75.4%, $p>0.05$), and a higher frequency of NK cells expressing the activating receptor NKG2C (48.0% vs 13.5%, $p<0.001$) (**Figure 5a**). A similar phenotype was generated using IL-2, IL-12, IL-18 and the cytokine cocktail, the latter resulting in particularly high frequencies of NKG2C+ NK cells within the CD49a+CXCR6+ population (64.2%) (**Supplementary Figure 4**). Upregulation of NKG2C on cytokine-generated CXCR6+ NK cells, was not associated with CD49a expression, as in contrast to liver NK cells, CD49a-CXCR6+ NK cells induced by IL-15 contained higher frequencies of NKG2C+ NK cells (35.0%) compared to CD49a-CXCR6- NK cells (18.9%, p<0.001) (**Figure 5b**).

Cytokine-induced peripheral blood CD49a+CXCR6+ NK cells produce high quantities of IFNγ

Following 12 hours culture with IL-12 a small increase in the percentages of CD49a+ (1.5% vs 3.3%, p<0.001) and CXCR6+ (4.2% vs 19.2%, p<0.0001) NK cells from rest can be seen. Consistent with their comparable phenotype to liver-resident CD49a+CXCR6+ NK cells, cytokine-induced CD49a+CXCR6+ NK cells produced similar quantities of IFNγ (**Figure 5c**). Cytokine-induced peripheral blood CXCR6+ NK cells failed to produce significant quantities of IFNγ unless they co-expressed CD49a (**Figure 5d**). However after six days of culture, over 80% of CXCR6+ NK cells were CD49a+ (unlike in the liver) (**Supplementary Figure 3).** Therefore, cytokine stimulation of peripheral blood NK cells can generate high frequencies of CD49a+CXCR6+ NK cells which are activated, express CD69 and produce high quantities of IFNγ (**Figure 5a, c)**.

DISCUSSION

We have shown that liver-resident CXCR6+ NK cells are immature (CD56^{bright}CD16^{low}) and are found in all individuals, comprising nearly two thirds of hepatic NK cells. While human CXCR6+ NK cells do not display features consistent with 'memory' as in mice, CXCR6 may play a role retaining NK cells within the liver via its interaction with the chemokine ligand 16 (CXCL16), expressed on sinusoidal endothelial cells, hepatocytes and cholangiocytes.[37] RNA sequencing has revealed reduced expression of markers of maturity and cytotoxicity.

Conversely, hepatic CD49a+ NK cells are only found in substantial frequencies in 10% of individuals, and may be even less frequent in a completely healthy population. The CD49a+ NK cell subset contains higher frequencies of KIR+ and NKG2C+ NK cells compared to the CD49a- subpopulation, suggesting some of these cells may have undergone previous clonal expansion. They also produce high quantities of IFNγ. While we did not stratify for CMV, no correlation was demonstrated between seropositivity and hepatic CD49a+ NK cell frequencies by Marqadt el at.[17]

We have demonstrated that cytokines can generate hyperfunctional CD49a+ NK cells from PBMCs in vitro, with a phenotype comparable to those found in the resting liver (CD56^{bright} CD69+ IFNγ+, with higher percentages of NKG2C+ NK cells compared to CD49a- NK subsets). CD49a is also known as very late activation antigen-1, and has previously been shown to be induced by IL-2.[38,39] We now show that this activation is associated with enhanced functionality and a phenotype associated with liver-residency. Therefore potentially in addition to having an activated phentoype, cytokine-induced CD49a+ NK cells may be adaptive, or a precursor of adaptive NK cells. However further experiments including additional stimulation would be useful to investigate this further.

The cytokine cocktail led to the greatest upregulation of CD49a in both PBMCs and hepatic MNCs. This may mimic events in vivo in which an inflammatory hepatic cytokine microenvironment, found in hepatitis or cancer, dominated by IL-1, IL-2, IL-6, IL-12, IL-15, IL-18, IFNα, IFNγ and TNFα/β,[40,41] may lead to the expansion of CD49a+ NK cells. Of the three patients in our cohort with significant enrichment of hepatic CD49a+ NK cells, one had hepatocellular carcinoma, one had aggressive colorectal cancer with synchronous lesions and bi-lobar liver metastases and the third had colorectal metastases extending to the resection margins, suggesting that high frequencies of CD49a+ NK cells are associated with more severe liver disease. The cytokine hyper-responsive behaviour observed in vitro in this subset may occur as a result of previous cytokine-priming and the adaptive qualities of liver-resident CD49a+ NK cells may therefore be driven through similar mechanisms to cytokine-induced memory-like NK cells generated in the blood.[26] It would be important to explore whether cytokine-induced CD49a+ NK cells generated in the peripheral blood display memory-like behaviour similar to that demonstrated for liver-resident CD49a+ NK cells,[17] or whether CD49a is a surface markers of cytokine-induced memory-like NK cells described by Romee et al.[26]

We show IL-2, IL-12 and IL-15 can upregulate CXCR6 on peripheral NK cells. This is likely to induce their migration towards and residence within tissues, but particularly the liver which is home to a major population of CXCR6+ NK cells and contains large numbers of CXCL16-expressing cells.[37] Both CXCR6+ and CD49a+ NK cells are associated with tissue-residency in organs other than the liver. However CXCR6+CD69+ NK cells from the spleen do not express CD49a, and CD49a+ NK cells from the lung are hypofunctional.[21,42] Furthermore dynamic flow assays mimicking hepatic sinusoids have shown that a small molecule inhibitor for CXCR6 can reduce migration of NK cells across the hepatic endothelium, indicating the relevance of this chemokine receptor for migration to the liver.[43] Cytokine-induced CXCR6+ NK cells are more activated than their hepatic counterparts, in terms of NKG2C expression, cytokine-induction and potential to produce high quantities of IFNγ where CD49a is co-expressed.

Interestingly, culture with the cytokine cocktail leads to a reduction in the frequencies of CXCR6+ NK cells within the hepatic NK cell population, and fails to expand the CXCR6+ population within PBMCs, in contrast to the individual influences of all four cytokines. Stimulation with the cytokine cocktail may lead to NK cell exhaustion due to persistent exposure to multiple activating cytokines and activation-induced NK cell apoptosis. Loss of activated cells within the culture may lead to a lower than expected frequency of CXCR6+ NK cells .

We have shown through culture with IL-12 or IL-15 it is possible to generate high frequencies of activated double-positive CD49a+CXCR6+ NK cells in the peripheral blood which display both markers of tissue residency (CD69) and phenotypic and functional similarities to liver-resident adaptive-like CD49a+ NK cells (NKG2C, IFNγ). This data also suggests cytokine signalling, in addition to CMV infection, can lead to expansion of NK cells expressing the adaptive marker NKG2C.[22–24] This transition may be supported by changes at a transcription factor level, for example IL-15 and TGFβ have recently been shown to induce transition of Eomes^{low} to Eomes^{high} NK cells.[29] However, CXCR6 was not upregulated under these conditions and T-bet is already highly expressed on the majority of CD49a- peripheral blood NK cells, suggesting other mechanisms may be important.[44]

It is therefore possible that in liver disease, in addition to clonal expansion of adaptive-like CD49a+ liver-resident NK cells, there is hepatic recruitment of newly generated CD49a+CXCR6+ NK cells, capable of releasing high levels of Th1 cytokines, induced by systemic inflammation in the peripheral blood including high levels of IL-12/IL-15. This process may be driven through IFNγ upregulation of CXCL16 in the liver. These findings may have important therapeutic applications. The generation of activated CXCR6+ NK cells in the peripheral blood that co-express CD49a and adopt an ‘adaptive’ phenotype, may allow hyperfunctional NK cells to be preferentially recruited to the liver, boosting the hepatic innate immune response to fight viruses and cancer, providing a basis for novel, locally acting immunotherapies for common hepatic disease.

MATERIALS AND METHODS

Patients

Patients were recruited from University Hospital Southampton NHS Foundation Trust. Liver tissue was obtained from the margin of 52 adults undergoing resection for liver metastases or primary liver cancer. Demographic data is displayed in **Supplementary Table 1**. Paired peripheral blood samples were obtained for 29 of the 52 patients, the remainder collected from individuals with haemochromatosis.

Isolation of mononuclear cells from human liver tissue

Tissue was infiltrated with chelating buffer (1x Phosphate Buffered Saline (PBS) (BioWhittaker, Belgium) 50ml, HEPES 28mg (Sigma, Poole, UK), EGTA 9.5mg (Sigma)) and perfusate collected. Cells were isolated from the liver parenchyma using collagenase digestion (Dulbecco's Modified Eagle Medium (DMEM) (Gibco®, Life Technologies™, UK) 50ml, TIV Collagenase 18mg (Sigma), calcium chloride 90µl (Sigma)) followed by mechanical disaggregation or mechanical disaggregation alone. Hepatic mononuclear cells (MNCs) and PBMCs were isolated using Ficoll-Paque™ density centrifugation (GE Healthcare, Sweden).

NK cell surface staining

Hepatic MNCs and PBMCs were analysed in parallel. Cells were incubated in Zombie Violet™ Fixable Viability Kit (Biolegend®, London, UK) for 15 minutes, then blocking buffer (10% human serum (HS) (Sigma) in FACS wash (PBS with 1% bovine serum albumin (BSA) (Sigma) and 0.1 % sodium azide (Sigma)) for 20 minutes prior to surface antibody staining: CD3 (UCHT1, PerCP, Biolegend®; UCHT1, BDV450, BD Biosciences, Oxford, UK; UCHT1, BV510, Biolegend®), CD56 (HCD56, PE-Cy7, Biolegend®), CD16 (3G8, APC-Cy7, Biolegend®), CD57 (HNK-1, APC, Biolegend®; NK-1, PE-CF594, BD Biosciences), CD161 (DX12, BV421, BD Biosciences), CD158a (HP-MA4, FITC, Biolegend®, KIR2DL1/S1/S3/S5), CD158b (CH-L, FITC, BD Biosciences, KIR2DL2/3; DX27, PerCP, Miltenyi Biotec, Guildford, UK, KIR2DL2/3), NKG2C (REA205, PE, Miltenyi Biotec; REA205, ViobrightFITC, Miltenyi Biotec; REA205, APC, Miltenyi Biotec), CD49a (SR84, PE, BD Biosciences), CD49b (AK-7, FITC, BD Biosciences), CXCR6 (K041E5, APC, Biolegend®; K041E5, PerCP/Cy5.5, Biolegend®). Cells were analysed using a three laser FACS Aria (BD Biosciences) flow cytometer. Gates were set using fluorescence minus one (FMO) controls. Data was analysed using FlowJo v.10.0 (Treestar, USA).

NK cell proliferation assays

Paired PBMCs and perfusate MNCs were resuspended in PBS/0.1% BSA to create a 2x cell solution. This was resuspended in Carboxyfluorecin succinimidyl ester (CFSE) staining solution (CellTrace^{TM} CFSE Cell Proliferation Kit) (Life Technologies^{TM}, Paisely, UK) to make a final CFSE concentration of 5µM and incubated for 10 minutes, 37°C. Staining was quenched with 5 volumes ice-cold Roswell Park Memorial Institute Medium (RPMI) 1640 + Glutamax (Gibco®, Life Technologies^{TM}) supplemented with 10% fetal bovine serum (Hyclone®, Thermoscienticic, Northumberland, UK), penicillin, streptomycin and glutamine (Gibco®, Life Technologies^{TM}) (R-10) and incubated for 5 minutes, 4°C. Cells were washed 3 times in R-10 then recounted. PBMCs and liver MNCs were incubated in R-10 supplemented with 5% HS (Sigma) in addition to Recombinant Human IL-2 100U/ml (PeproTech, London, UK), IL-12 10ng/ml (PeproTech), IL-15 25ng/ml (R&D Systems, Oxford, UK), IL-18 100ng/ml (Medical and Biological Laboratories, Japan), or a cocktail of all four for 6 days. Media and cytokines were changed every 2-3 days. A CFSE FMO was included. On day 0 and 6 PBMCs and liver MNCs underwent staining with Zombie Violet^{TM} Fixable Viability Kit (Biolegend®), CD3-BV510 (Biolegend®), CD56-PECy7 (Biolegend®), NKG2C-APC (Miltenyi Biotec), CXCR6-PerCP/Cy5.5 (Biolegend®) and CD49a-PE (BD Biosciences).

NK cell purification and stimulation with IL-12 and IL-15

Freshly isolated PBMCs from individuals with haemochromatosis were passed through a 70µm filter prior to counting, then centrifuged at 300g for 10 minutes and resuspended in NK cell isolation buffer (NKIB) (40µl per 10^7 cells) (250mM Ethylene diamine tetraacetic Acid 2ml, pH 8, BSA 1.25g, 248ml PBS) and NK cell biotin-antibody cocktail (10µl per 10^7 cells) (Human NK cell isolation kit, Miltenyi Biotec) and incubated for 5 minutes, 4°C. Cells were resuspended in 30µl per 10^7 cells NKIB and NK cell micro-bead cocktail (20µl per 10^7 cells) (Human NK cell isolation kit, Miltenyi Biotec) and incubated for 10 minutes, 4°C. The cell suspension was placed onto the LS column (Miltenyi Biotec) and unlabelled NK cells collected. The column was rinsed with a further 3ml NKIB and cell suspension collected. Purified NK cells were cultured for 12 hours at 0.2×10^6 cell / 200µl R-10 supplemented with 5% HS alone or with IL-12 10ng/ml, or IL-15 25ng/m prior to surface staining with CD3-BV510, CD56-PE-Cy7, CXCR6-PerCP/Cy5.5 and CD49a-PE as above.

NK cell intracellular interferon gamma and tumour necrosis factor staining

PBMCs and liver MNCs were stimulated for 12 hours with IL-12 10ng/ml (PeproTech) or IL-15 1ng/ml (R&D Systems) to examine IFNγ and TNFα production respectively. An unstimulated control was included. BD GolgiStop^{TM} (BD Biosciences) was added (4µl/6ml culture medium) for the last 4 hours. Surface staining was performed for CD3-BV510 (Biolegend®), CD56-PE-Cy7 (Biolegend®), CXCR6-PerCP/Cy5.5 (Biolegend®) and CD49a-PE (BD Biosciences). Cells were fixed and permeabilised (BD Cytofix/Cytoperm^{TM} Plus Kit, BD Biosciences) prior to incubation with IFNγ (B27, APC, Biolegend®) or TNFα (MAb11, FITC, Biolegend®).

RNA sequencing

Hepatic CXCR6+ and CXCR6- NK cells were sorted using fluorescence-activated cell sorting, gating on live CD3-CD56+CXCR6+ and CD3-CD56+CXCR6- lymphocytes. Total RNA was isolated using TRIzol® reagent (Life Technologies^{TM}) and digested with RNase-Free DNase-I. Quantity and quality of extracted RNA were analysed using the Fragment Analyser (Advanced Analytical) and NanoDrop® ND-1000 Spectrophotometer (Thermo Scientific NanoDrop Technologies, USA). 50ng of each total RNA was used as starting material. TruSeq Stranded Total RNA Library Prep Kit with Ribo-Zero Human/Mouse/Rat (Illumina Cat. N° RS122-2201) was used to prepare samples. Accurate quantitation of cDNA libraries was performed using the QuantiFluorTM dsDNA System (Promega, Germany) and the size range of cDNA libraries determined using the Fragment Analyser (280bp). cDNA libraries were amplified and sequenced using cBot and HiSeq 2000 (llumina) (SR, 50bp, ca. 30 million reads/sample). Sequence images were transformed with Illumina software BaseCaller, which were demultiplexed with CASAVA (v.1.8.2). Quality checks were performed via FastQC (Babraham Bioinformatics).

Sequenced reads were mapped against the human genome (hg38) using STAR (version 020201)[45] with parameters --outSAMtype BAM SortedByCoordinate --outFilterMismatchNmax 2. Read counts per gene were examined using featureCount (v.1.5.0-p1).[46] Normalization of read counts to the library size, estimation of dispersions and testing for differentially expressed genes based on a statistical test assuming negative binomial data distribution were computed in the R/Bioconductor environment (v.2.15.2) loading DESeq2 (1.14.1) and biomaRt (2.14.0) packages.[31,47,48] Significant genes were determined as log2 fold change (log2FC) <1 or >−1, base mean <1000, and false discovery rate-corrected p-value <0.05 with multiple testing correction according to Benjamini and

Hochberg. The top 75 differetially expressed genes were used to construct a heat map . Euclidian distance matrix was also calculated using DeSeq2. Data generated conformed to *MIAME* standards and was submitted to the Gene Expression Omnibus database.

Ethical approval

Ethical approval to collect paired peripheral blood and liver tissue was granted by the Wales Research Ethics Committee (REC No. 13/WA/0329). Ethical approval to collect peripheral blood samples from haemochromatosis patients was granted by the South Central Hampshire Research Ethics Committee (REC No. 06/Q1701/120). Informed consent of all participants was obtained.

ACKNOWLEDGEMENTS

We would like to acknowledge the Medical Research Council (MRC) who funded this work and the support of the National Institute for Health Research (NIHR) Clinical Research Network (NIHR No. 17075) and the NIHR Wellcome Trust Research Facility.

CONFLICTS OF INTEREST

The authors declare no commercial or financial conflict of interest.

REFERENCES

1. Norris S, Collins C, Doherty DG, Smith F, McEntee G, Traynor O, et al. Resident human hepatic lymphocytes are phenotypically different from circulating lymphocytes. *J Hepatol*. 1998;28(1):84–90.
2. Doherty DG, O’Farrelly C. Innate and adaptive lymphoid cells in the human liver. *Immunol Rev*. 2000;174:5–20.
3. Khakoo SI, Thio CL, Martin MP, Brooks CR, Gao X, Astemborski J, et al. HLA and NK cell inhibitory receptor genes in resolving hepatitis C virus infection. *Science*. 2004;305(5685):872–4.
4. Knapp S, Warshow U, Hegazy D, Brackenbury L, Guha IN, Fowell A, et al. Consistent beneficial effects of killer cell immunoglobulin-like receptor 2DL3 and group 1 human leukocyte antigen-C following exposure to hepatitis C virus. *Hepatology*. 2010;51(4):1168–75.
5. Vidal-Castiñeira JR, López-Vázquez A, Díaz-Peña R, Alonso-Arias R, Martínez-Borra J, Pérez R, et al. Effect of killer immunoglobulin-like receptors in the response to combined treatment in patients with chronic hepatitis C virus infection. *J Virol*. 2010;84(1):475–81.
6. Gao X, Jiao Y, Wang L, Liu X, Sun W, Cui B, et al. Inhibitory KIR and specific HLA-C gene combinations confer susceptibility to or protection against chronic hepatitis B. *Clin Immunol*. 2010;137(1):139–46.
7. Kumar V, Kato N, Urabe Y, Takahashi A, Muroyama R, Hosono N, et al. Genome-wide association study identifies a susceptibility locus for HCV-induced hepatocellular carcinoma. *Nat Genet*. 2011;43(5):455–8.
8. Pembroke T, Christian A, Jones E, Hills RK, Wang ECY, Gallimore AM, et al. The paradox of NKp46+ natural killer cells: drivers of severe hepatitis C virus-induced

pathology but in-vivo resistance to interferon α treatment. *Gut*. 2013;1–10.

9. Ahlenstiel G, Titerence RH, Koh C, Edlich B, Feld JJ, Rotman Y, et al. Natural killer cells are polarized toward cytotoxicity in chronic hepatitis C in an interferon-alfa-dependent manner. *Gastroenterology*. 2010;138(1):325-35-2.

10. Cai L, Zhang Z, Zhou L, Wang H, Fu J, Zhang S, et al. Functional impairment in circulating and intrahepatic NK cells and relative mechanism in hepatocellular carcinoma patients. *Clin Immunol*. 2008;129(3):428–37.

11. O'Leary JG, Goodarzi M, Drayton DL, von Andrian UH. T cell- and B cell-independent adaptive immunity mediated by natural killer cells. *Nat Immunol*. 2006;7(5):507–16.

12. Paust S, Gill HS, Wang B-Z, Flynn MP, Moseman EA, Senman B, et al. Critical role for the chemokine receptor CXCR6 in NK cell-mediated antigen-specific memory of haptens and viruses. *Nat Immunol*. 2010;11(12):1127–35.

13. Peng H, Jiang X, Chen Y, Sojka DK, Wei H, Gao X, et al. Liver-resident NK cells confer adaptive immunity in skin-contact inflammation. *J Clin Invest*. 2013;123(4).

14. Sun JC, Beilke JN, Lanier LL. Adaptive immune features of natural killer cells. *Nature*. 2009;457(7229):557–61.

15. Sun JC, Madera S, Bezman NA, Beilke JN, Kaplan MH, Lanier LL. Proinflammatory cytokine signaling required for the generation of natural killer cell memory. *J Exp Med*. 2012;209(5):947–54.

16. Reeves RK, Li HH, Jost S, Blass E, Li HH, Schafer JL, et al. Antigen-specific NK cell memory in rhesus macaques. *Nat Immunol*. 2015;16(9):927–32.

17. Marquardt N, Béziat V, Nyström S, Hengst J, Ivarsson MA, Kekäläinen E, et al. Cutting Edge: Identification and Characterization of Human Intrahepatic CD49a+ NK Cells. *J Immunol*. 2015;194(6):2467–71.

18. Hudspeth K, Donadon M, Cimino M, Pontarini E, Tentorio P, Preti M, et al. Human liver-resident CD56(bright)/CD16(neg) NK cells are retained within hepatic sinusoids

via the engagement of CCR5 and CXCR6 pathways. *J Autoimmun*. 2016;66:40–50.

19. Harmon C, Robinson MW, Fahey R, Whelan S, Houlihan DD, Geoghegan J, et al. Tissue-resident Eomes hi T-bet lo CD56 bright NK cells with reduced proinflammatory potential are enriched in the adult human liver. *Eur J Immunol*. 2016;46(9):2111–20.

20. Stegmann KA, Robertson F, Hansi N, Gill U, Pallant C, Christophides T, et al. CXCR6 marks a novel subset of T-betloEomeshi natural killer cells residing in human liver. *Sci Rep*. 2016;6:26157.

21. Lugthart G, Melsen JE, Vervat C, van Ostaijen-ten Dam MM, Corver WE, Roelen DL, et al. Human Lymphoid Tissues Harbor a Distinct CD69 + CXCR6 + NK Cell Population. *J Immunol*. 2016;197(1):78–84.

22. Gumá M, Angulo A, Vilches C, Gómez-Lozano N, Malats N, López-Botet M. Imprint of human cytomegalovirus infection on the NK cell receptor repertoire. *Blood*. 2004;104(12):3664–71.

23. Gumá M, Cabrera C, Erkizia I, Bofill M, Clotet B, Ruiz L, et al. Human Cytomegalovirus Infection Is Associated with Increased Proportions of NK Cells That Express the CD94/NKG2C Receptor in Aviremic HIV-1–Positive Patients. *J Infect Dis*. 2006;194(1):38–41.

24. Lopez-Vergès S, Milush JM, Schwartz BS, Pando MJ, Jarjoura J, York VA, et al. Expansion of a unique CD57^{+}NKG2Chi natural killer cell subset during acute human cytomegalovirus infection. *Proc Natl Acad Sci U S A*. 2011;108(36):14725–32.

25. Cooper MA, Elliott JM, Keyel PA, Yang L, Carrero JA, Yokoyama WM. Cytokine-induced memory-like natural killer cells. *Proc Natl Acad Sci U S A*. 2009;106(6):1915–9.

26. Romee R, Schneider SE, Leong JW, Chase JM, Keppel CR, Sullivan RP, et al. Cytokine activation induces human memory-like NK cells. *Blood*. 2012;120(24):4751–60.

27. Romee R, Rosario M, Berrien-Elliott MM, Wagner JA, Jewell BA, Schappe T, et al.

Cytokine-induced memory-like natural killer cells exhibit enhanced responses against myeloid leukemia. *Sci Transl Med*. 2016;8(357).

28. Lassen MG, Lukens JR, Dolina JS, Brown MG, Hahn YS. Intrahepatic IL-10 maintains NKG2A+Ly49- liver NK cells in a functionally hyporesponsive state. *J Immunol*. 2010;184(5):2693–701.

29. Cuff AO, Robertson FP, Stegmann KA, Pallett LJ, Maini MK, Davidson BR, et al. Eomes hi NK Cells in Human Liver Are Long-Lived and Do Not Recirculate but Can Be Replenished from the Circulation. *J Immunol*. 2016;197(11):4283–91.

30. Berrien-Elliott MM, Wagner JA, Fehniger TA. Human Cytokine-Induced Memory-Like Natural Killer Cells. *J Innate Immun*. 2015;7(6):563–71.

31. Love MI, Huber W, Anders S. Moderated estimation of fold change and dispersion for RNA-seq data with DESeq2. *Genome Biol*. 2014;15(12):550.

32. Matza D, Badou A, Jha MK, Willinger T, Antov A, Sanjabi S, et al. Requirement for AHNAK1-mediated calcium signaling during T lymphocyte cytolysis. *Proc Natl Acad Sci*. 2009;106(24):9785–90.

33. Lui-Roberts WWY, Stinchcombe JC, Ritter AT, Akhmanova A, Karakesisoglou I, Griffiths GM. Cytotoxic T lymphocyte effector function is independent of nucleus-centrosome dissociation. *Eur J Immunol*. 2012;42(8):2132–41.

34. Yeang HXA, Lin Y, Malkova ON, Yang L, Piersma SJ, Miner C, et al. Human liver contains two populations of NK cells based on CD49e expression. *J Immunol*. 2016;196(1 Supplement):194.7-194.7.

35. Fu B, Wang F, Sun R, Ling B, Tian Z, Wei H. CD11b and CD27 reflect distinct population and functional specialization in human natural killer cells. *Immunology*. 2011;133(3):350–9.

36. Rölle A, Halenius A, Ewen E-M, Cerwenka A, Hengel H, Momburg F. CD2-CD58 interactions are pivotal for the activation and function of adaptive natural killer cells

in human cytomegalovirus infection. *Eur J Immunol*. 2016;46(10):2420–5.

37. Heydtmann M, Lalor PF, Eksteen JA, Hübscher SG, Briskin M, Adams DH. CXC chemokine ligand 16 promotes integrin-mediated adhesion of liver-infiltrating lymphocytes to cholangiocytes and hepatocytes within the inflamed human liver. *J Immunol*. 2005;174(2):1055–62.

38. Hemler ME, Jacobson JG, Brenner MB, Mann D, Strominger JL. VLA-1: a T cell surface antigen which defines a novel late stage of human T cell activation. *Eur J Immunol*. 1985 May [cited 2017 May 6];15(5):502–8.

39. Pérez-Villar JJ, Melero I, Gismondi A, Santoni A, López-Botet M. Functional analysis of α1β1 integrin in human natural killer cells. *Eur J Immunol*. 1996 Sep [cited 2017 May 6];26(9):2023–9.

40. Tilg H. Cytokines and liver diseases. *Can J Gastroenterol*. 2001;15(10):661–8.

41. Ramadori G, Armbrust T. Cytokines in the liver. *Eur J Gastroenterol Hepatol*. 2001;13(7):777–84.

42. Marquardt N, Kekäläinen E, Chen P, Kvedaraite E, Wilson JN, Ivarsson MA, et al. Human lung natural killer cells are predominantly comprised of highly differentiated hypofunctional CD69 − CD56 dim cells. *J Allergy Clin Immunol*. 2017 Apr [cited 2017 May 6];139(4):1321–1330.e4.

43. Parker R, Weston CJ, Adams DH. CXCR6 and CXCL16 in liver disease. *Lancet*. 2013;381:S83.

44. Knox JJ, Cosma GL, Betts MR, McLane LM. Characterization of T-bet and eomes in peripheral human immune cells. *Front Immunol*. 2014;5:217.

45. Dobin A, Davis CA, Schlesinger F, Drenkow J, Zaleski C, Jha S, et al. STAR: ultrafast universal RNA-seq aligner. *Bioinformatics*. 2013;29(1):15–21.

46. Liao Y, Smyth GK, Shi W. featureCounts: an efficient general purpose program for assigning sequence reads to genomic features. *Bioinformatics*. 2014;30(7):923–30.

47. Anders S, Huber W. Differential expression analysis for sequence count data. *Genome Biol*. 2010;11(10):R106.

48. Durinck S, Spellman PT, Birney E, Huber W. Mapping identifiers for the integration of genomic datasets with the R/Bioconductor package biomaRt. *Nat Protoc*. 2009;4(8):1184–91.

FIGURE LEGENDS

Figure 1. a) Representative flow cytometry plots showing gating strategy and individual frequencies of CD49a+ and CXCR6+ NK cell populations within the peripheral blood and hepatic perfusate. **b)** A comparison of the frequency of CD49a+ (n=20) and CXCR6+ (n=22) NK cells within the peripheral blood and hepatic perfusate (paired samples). Dot plots display individual values. (Wilcoxon matched pairs test). **c)** Distribution of frequencies of CD49a+ (n=35) and CD49a+CXCR6+ (n=27) NK cells within the hepatic lymphocyte population. Dot plot displays individual values and median. Individuals with high frequencies of CD49a+ NK cells are plotted with a cross. Representative flow cytometry plots gated on NK cells showing examples of individuals with average and high frequencies of CD49a+CXCR6+ NK cells. **d)** Frequencies of CD49a+CXCR6+, CD49a+CXCR6-, CD49a-CXCR6+ and CD49a-CXCR6- NK cell subsets in the human liver (n=27). Dot plots display individual values and median. **e)** Comparison of frequency of CD16 (n=12), CD57 (n=12), CD69 (n=11), NKG2C (n=22) and KIR+ (n=9) NK cells between liver-resident subpopulations CD49a+CXCR6+, CD49a+CXCR6-, CD49a-CXCR6+ and CD49a-CXCR6- (Wilcoxon matched pairs test). Representative flow cytometry plots gated on CD49a+/- and CXCR6+/- NK cells showing expression of CD16, CD57, CD69, NKG2C and KIR. **f)** Percentage of IFNγ+ (n=7) and TNFα+ (n=6) NK cells within the hepatic CD49a+CXCR6+, CD49a+CXCR6-, CD49a-CXCR6+ and CD49a-CXCR6- NK cell populations following stimulation with IL-12 10ng/ml and IL-15 1ng/ml for 12 hours respectively. Dot plots display individual values and median. (Wilcoxon matched pairs test). Representative flow cytometry plots gated on CD49a+/- and CXCR6+/- NK cells showing IFNγ and TNFα production. $p<0.05$*, $p<0.01$**, $p<0.001$***, $p<0.0001$****.

Figure 2. RNA-sequencing of CXCR6+ and CXCR6- NK cells isolated from the liver perfusate from three patients, resulting in six paired samples (s77 + s78, s102 + s107, s108 + s109). All three patients had undergone resection for colorectal metastases and had either a normal background liver or mild steatosis. Genes with a p value (adjusted for multiple comparisons according to Benjamini Hochberg) of <0.05 were analysed using: **a)** Euclidian distance matrix displaying the overall similarity between samples, **b)** a heat map displaying the top 75 differentially expressed genes in CXCR6+ and CXCR6- NK cells, and **c)** differential expression of other selected genes of interest between CXCR6+ and CXCR6- NK cells.

Figure 3. **a)** Representative flow cytometry plots gated on NK cells, individual frequencies shown. **b)** Percentage of CD49a+ and CXCR6+ NK cells in the peripheral blood at rest (day 0) and following incubation with IL-2, IL-12, IL-15, IL-18 and the cytokine cocktail (n=8). Dot plots display individual values. (Wilcoxon matched pairs test). **c)** Percentage of CD49a+CXCR6+ NK cells in the liver at rest (day 0) and following incubation with IL-2, IL-12, IL-15, IL-18 and a cytokine cocktail at day six. Median percentages are shown. Dot plots display individual values. **d)** Day six CFSE MFI of hepatic CD49a+ vs CXCR6+ NK cells following culture with IL-2, IL-12, IL-15, IL-18 and the cytokine cocktail (n=8). Dot plots display individual values and median (Wilcoxon matched pairs test). Representative flow cytometry histograms from one individual showing CFSE MFI of CD49a+ and CXCR6+ NK cells at day six following culture with IL-15. $p<0.05$*, $p<0.01$**.

Figure 4. **a)** Representative flow cytometry plots gated on NK cells, individual frequencies shown. **b)** Percentage of CD49a+ and CXCR6+ NK cells in the peripheral blood at rest (day 0) and following incubation with IL-2, IL-12, IL-15, IL-18 and the cytokine cocktail (n=9). Dot plots display individual values. (Wilcoxon matched pairs test). **c)** Absolute number of CD49a+/- and CXCR6+/- NK cells at rest (day 0) and following incubation with IL-2, IL-12, IL-15, IL-18 and the cytokine cocktail. (n=9). Dot plots display individual values. Median absolute cell numbers shown in table below. **d)** Percentage of CD49a+CXCR6+ NK cells in the peripheral blood at rest (day 0) and following incubation with IL-2, IL-12, IL-15, IL-18 and a cytokine cocktail at day six. Median percentages are shown. Dot plots display individual values. **e)** Day six CFSE MFI of CD49a+ vs CXCR6+ NK cells in the peripheral blood following culture with IL-2, IL-12, IL-15, IL-18 and the cytokine cocktail (n=8). Dot plots display individual values and median (Wilcoxon matched pairs test). Representative flow cytometry histograms from one individual showing CFSE MFI of CD49a+ and CXCR6+ NK cells at day six following culture with IL-15. **f)** Frequency of CD49a+ and CXCR6+ NK cells at rest and following a 12 hours culture with media only, IL-12 10ng/ml or IL-15 25ng/ml using purified NK cells (n=12). Dot plots display median. (Wilcoxon matched pairs test). $p<0.05$*, $p<0.01$**, $p<0.001$***

Figure 5. **a)** A comparison of the frequencies of CD69+ (n=11 liver, n=6 cytokine-induced) and NKG2C+ (n=21 liver, n=8 cytokine-induced) NK cells between CD49a+CXCR6+ populations isolated from the liver and those generated in the peripheral blood following six days of culture with IL-15. Dot plots display individual values and median. (Mann Whitney U test). **b)** A comparison of the frequencies of CD56^{bright} (n=8), CD69+ (n=6) and NKG2C+ (n=8) NK cells within CD49a+CXCR6+, CD49a+CXCR6-, CD49a-CXCR6+, CD49a-CXCR6- NK subsets generated in the peripheral blood following six days of culture with IL-15. Dot plots display individual values and median. (Wilcoxon matched pairs test). **c)** A comparison of the frequency of IFNγ+ NK cells (n=7 liver, n=15 cytokine-induced) between CD49a+CXCR6+ populations isolated from the liver and those generated in the peripheral blood following stimulation with IL-12 for 12 hours. Dot plots display individual values and median. (Mann Whitney U test). **d)** A comparison of the frequency of IFNγ+ NK cells (n=15) between CD49a+CXCR6+, CD49a+CXCR6-, CD49a-CXCR6+, CD49a-CXCR6- NK subsets generated in the peripheral blood following stimulation with IL-12 for 12 hours. Dot plots display individual values and median. (Wilcoxon matched pairs test). $p<0.05$*, $p<0.001$***.

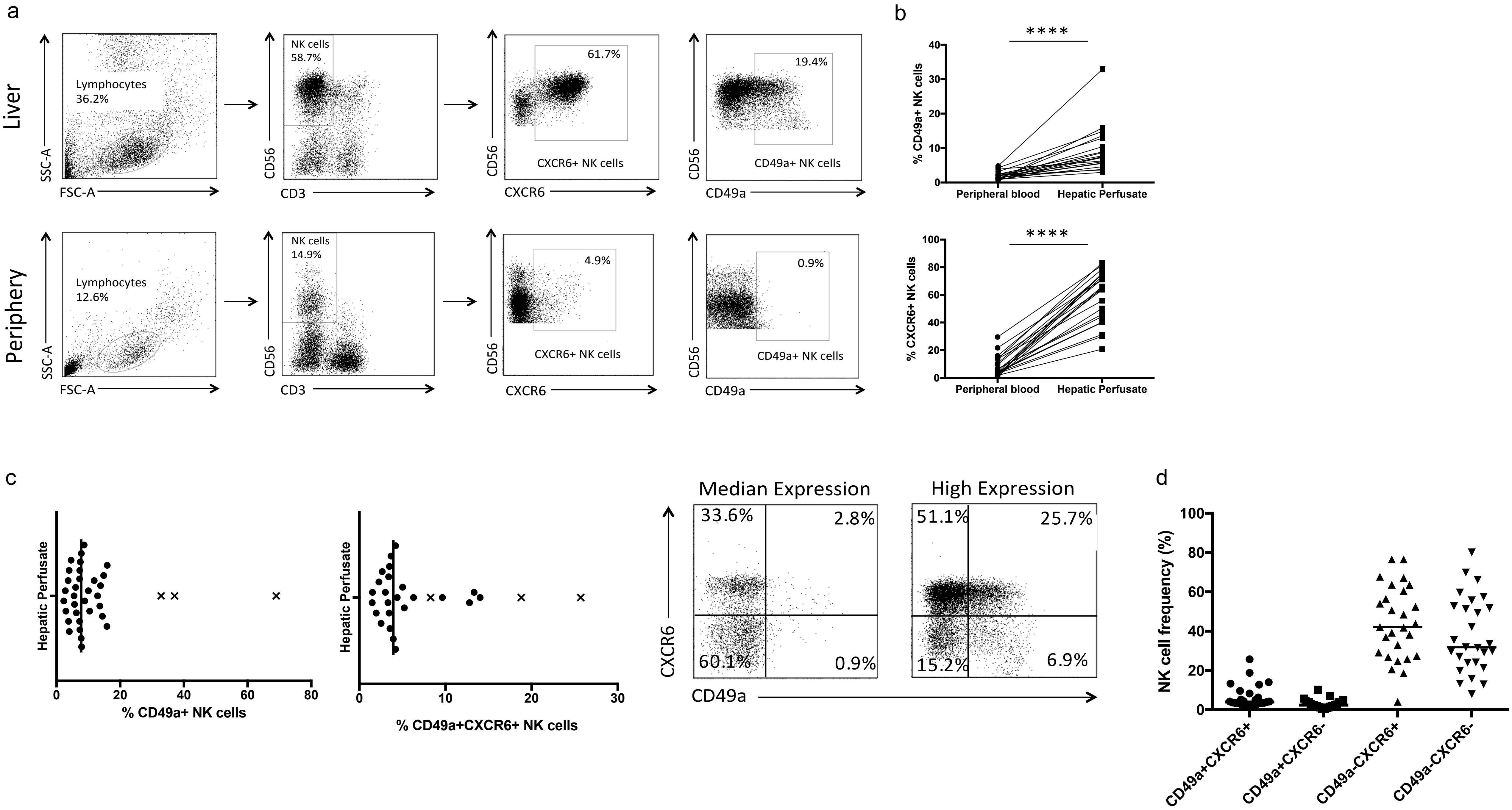
a
Liver
Periphery
SSC-A
FSC-A
Lymphocytes 36.2%
Lymphocytes 12.6%
CD56
CD3
NK cells 58.7%
NK cells 14.9%
CXCR6
61.7%
4.9%
CXCR6+ NK cells
CD49a
19.4%
0.9%
CD49a+ NK cells
b
****
% CD49a+ NK cells
% CXCR6+ NK cells
0
10
20
30
40
60
80
100
Peripheral blood
Hepatic Perfusate
c
Hepatic Perfusate
% CD49a+ NK cells
% CD49a+CXCR6+ NK cells
Median Expression
High Expression
33.6%
2.8%
60.1%
0.9%
51.1%
25.7%
15.2%
6.9%
CXCR6
CD49a
d
NK cell frequency (%)
CD49a+CXCR6+
CD49a+CXCR6-
CD49a-CXCR6+
CD49a-CXCR6-

e

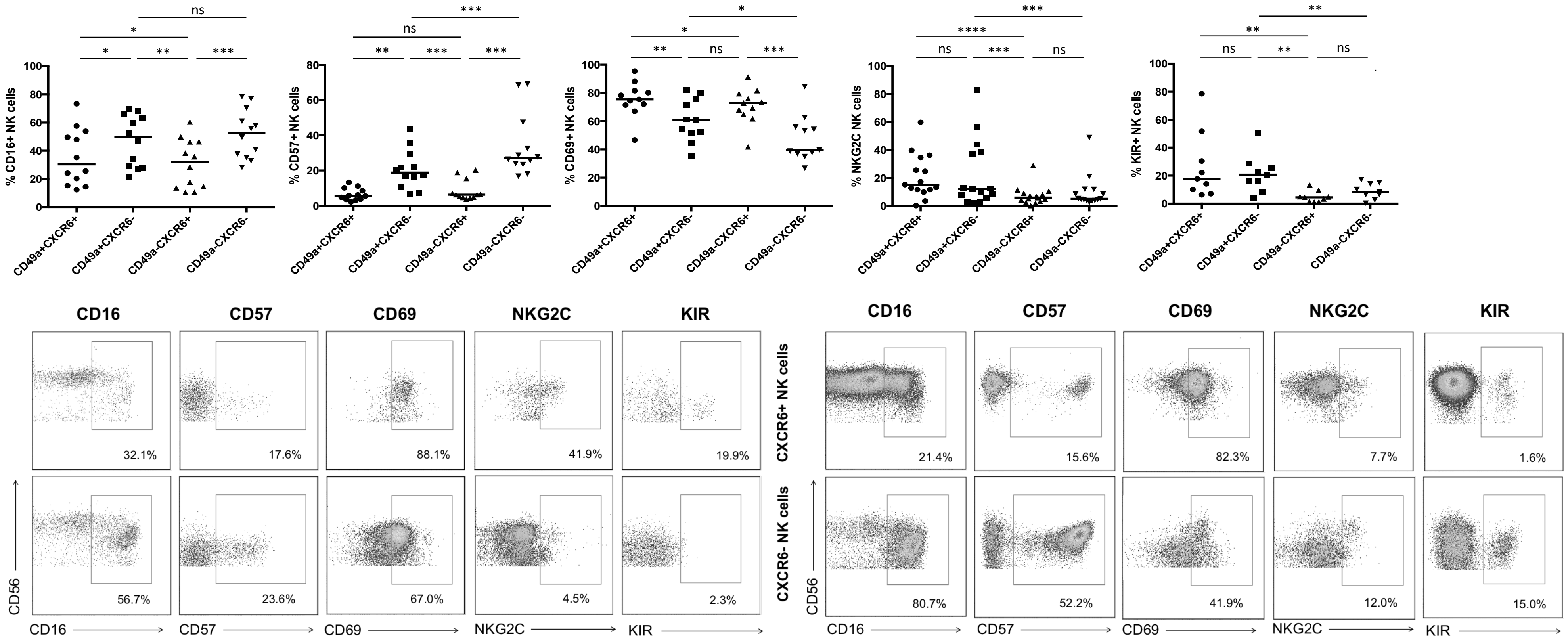

% CD16+ NK cells
% CD57+ NK cells
% CD69+ NK cells
% NKG2C NK cells
% KIR+ NK cells
CD49a+CXCR6+
CD49a+CXCR6-
CD49a-CXCR6+
CD49a-CXCR6-
ns
*
**
***
****
CD16
CD57
CD69
NKG2C
KIR
CD49a+ NK cells
CD49a- NK cells
CXCR6+ NK cells
CXCR6- NK cells
32.1%
17.6%
88.1%
41.9%
19.9%
56.7%
23.6%
67.0%
4.5%
2.3%
21.4%
15.6%
82.3%
7.7%
1.6%
80.7%
52.2%
41.9%
12.0%
15.0%
CD56

f

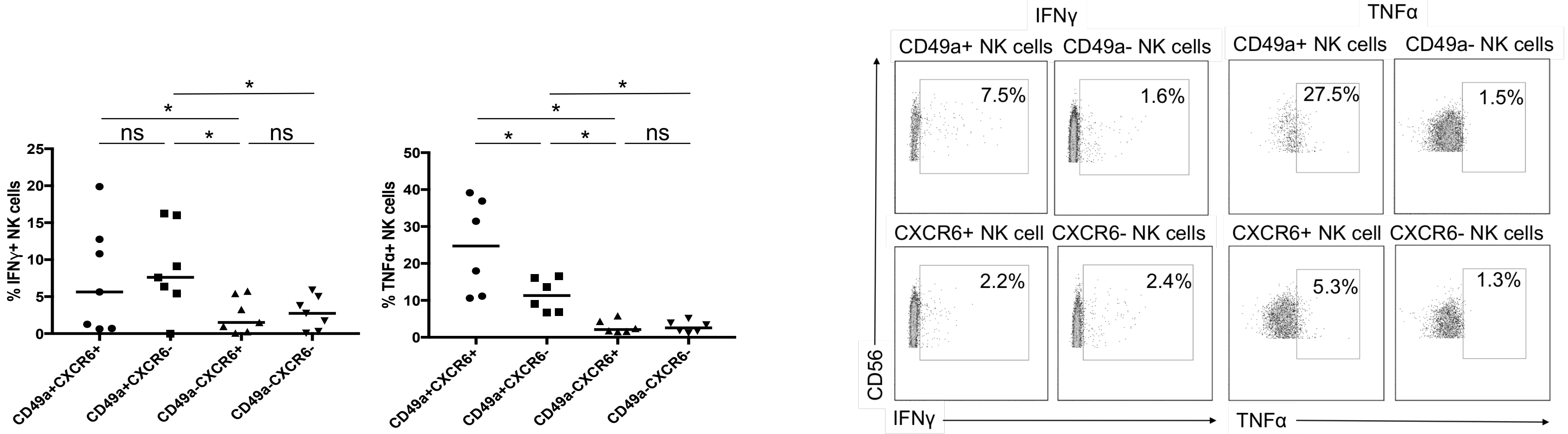

% IFNγ+ NK cells
% TNFα+ NK cells
CD49a+CXCR6+
CD49a+CXCR6-
CD49a-CXCR6+
CD49a-CXCR6-
ns
*
IFNγ
TNFα
CD49a+ NK cells
CD49a- NK cells
7.5%
1.6%
27.5%
1.5%
CXCR6+ NK cell
CXCR6- NK cells
2.2%
2.4%
5.3%
1.3%
CD56

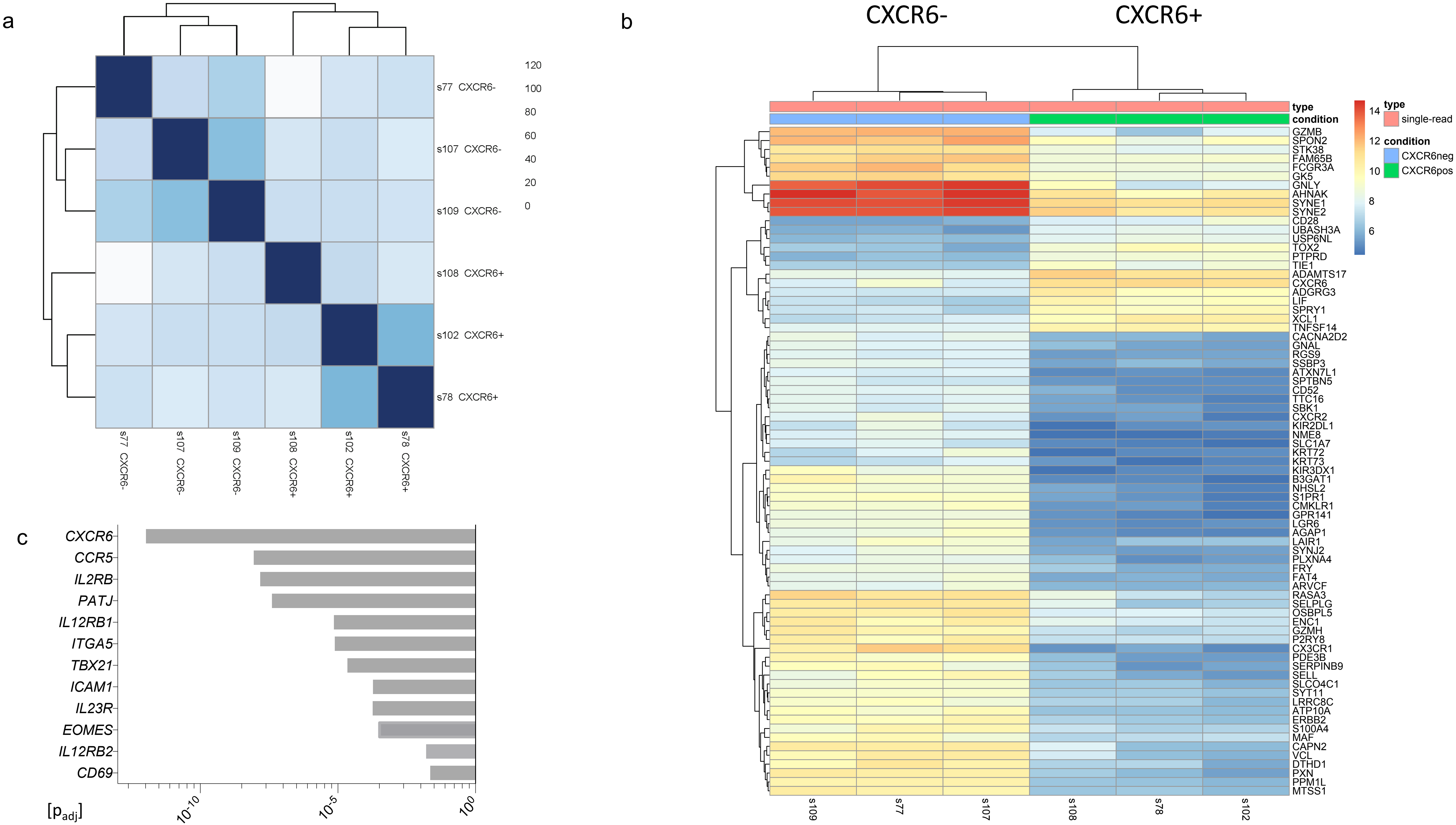
a
s77 CXCR6-
s107 CXCR6-
s109 CXCR6-
s108 CXCR6+
s102 CXCR6+
s78 CXCR6+
120
100
80
60
40
20
0
b
CXCR6-
CXCR6+
type
condition
14
12
10
8
6
type
single-read
condition
CXCR6neg
CXCR6pos
GZMB
SPON2
STK38
FAM65B
FCGR3A
GK5
GNLY
AHNAK
SYNE1
SYNE2
CD28
UBASH3A
USP6NL
TOX2
PTPRD
TIE1
ADAMTS17
CXCR6
ADGRG3
LIF
SPRY1
XCL1
TNFSF14
CACNA2D2
GNAL
RGS9
SSBP3
ATXN7L1
SPTBN5
CD52
TTC16
SBK1
CXCR2
KIR2DL1
NME8
SLC1A7
KRT72
KRT73
KIR3DX1
B3GAT1
NHSL2
S1PR1
CMKLR1
GPR141
LGR6
AGAP1
LAIR1
SYNJ2
PLXNA4
FRY
FAT4
ARVCF
RASA3
SELPLG
OSBPL5
ENC1
GZMH
P2RY8
CX3CR1
PDE3B
SERPINB9
SELL
SLCO4C1
SYT11
LRRC8C
ATP10A
ERBB2
S100A4
MAF
CAPN2
VCL
DTHD1
PXN
PPM1L
MTSS1
s109
s77
s107
s108
s78
s102
c
CXCR6
CCR5
IL2RB
PATJ
IL12RB1
ITGA5
TBX21
ICAM1
IL23R
EOMES
IL12RB2
CD69
[p_adj]
10^-10
10^-5
10^0

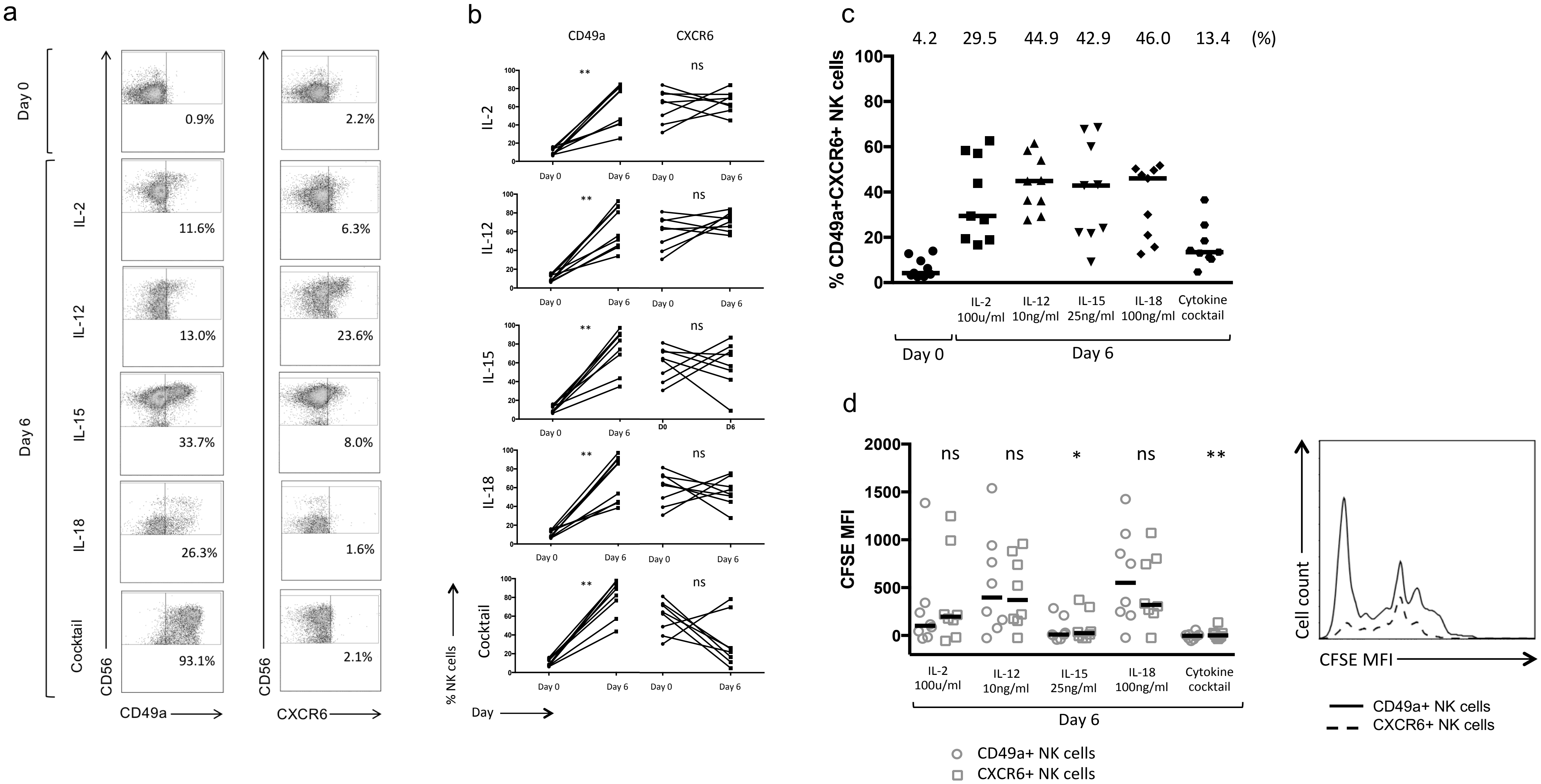
a
Day 0
Day 6
IL-2
IL-12
IL-15
IL-18
Cocktail
CD56
CD49a
CXCR6
0.9%
2.2%
11.6%
6.3%
13.0%
23.6%
33.7%
8.0%
26.3%
1.6%
93.1%
2.1%
b
CD49a
CXCR6
**
ns
Day 0
Day 6
D0
D6
% NK cells
Day
c
4.2
29.5
44.9
42.9
46.0
13.4
(%)
% CD49a+CXCR6+ NK cells
IL-2 100u/ml
IL-12 10ng/ml
IL-15 25ng/ml
IL-18 100ng/ml
Cytokine cocktail
Day 0
Day 6
d
CFSE MFI
ns
ns
*
ns
**
IL-2 100u/ml
IL-12 10ng/ml
IL-15 25ng/ml
IL-18 100ng/ml
Cytokine cocktail
Day 6
CD49a+ NK cells
CXCR6+ NK cells
Cell count
CFSE MFI
CD49a+ NK cells
CXCR6+ NK cells

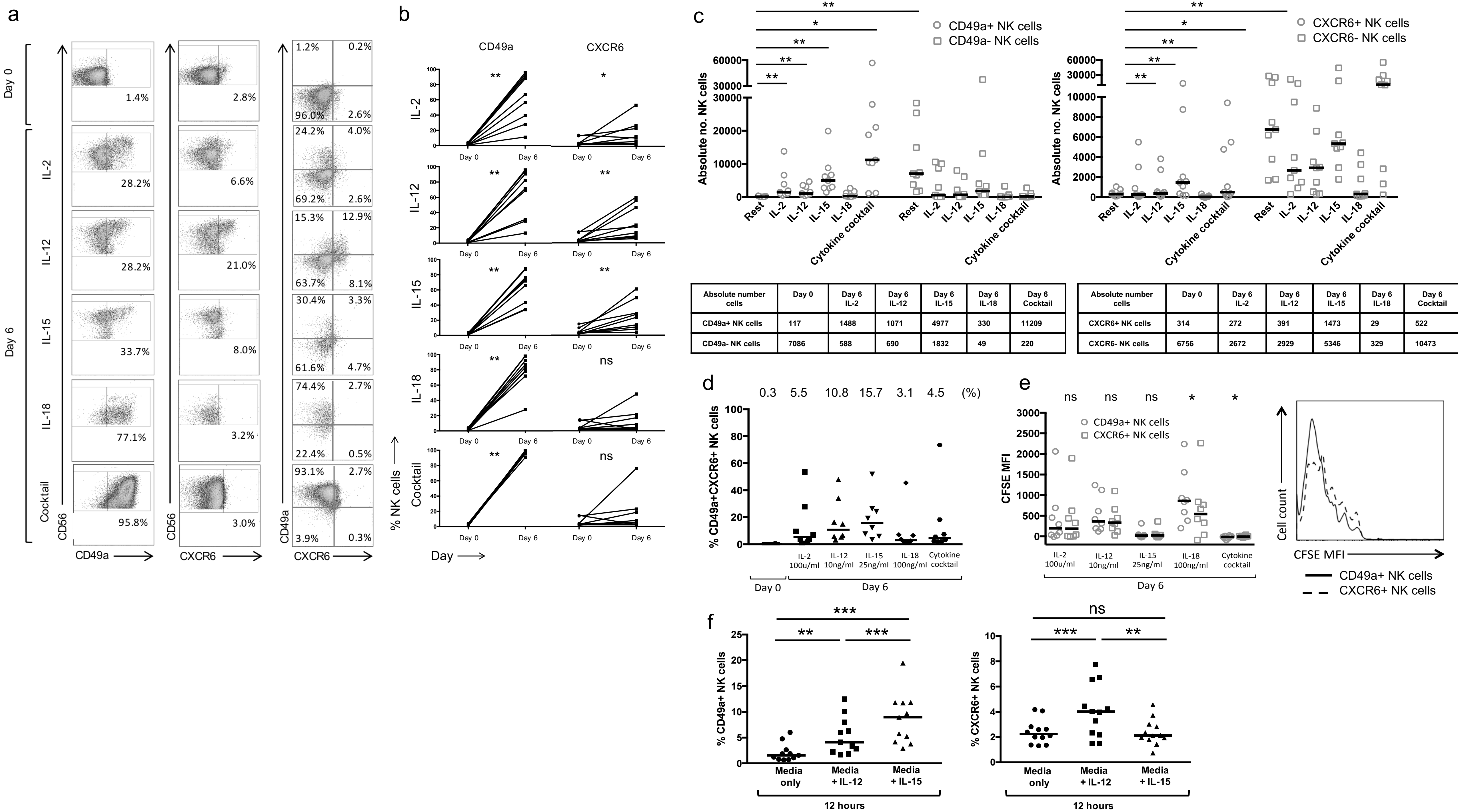

Absolute number cells	Day 0	Day 6 IL-2	Day 6 IL-12	Day 6 IL-15	Day 6 IL-18	Day 6 Cocktail
CD49a+ NK cells	117	1488	1071	4977	330	11209
CD49a- NK cells	7086	588	690	1832	49	220

Absolute number cells	Day 0	Day 6 IL-2	Day 6 IL-12	Day 6 IL-15	Day 6 IL-18	Day 6 Cocktail
CXCR6+ NK cells	314	272	391	1473	29	522
CXCR6- NK cells	6756	2672	2929	5346	329	10473

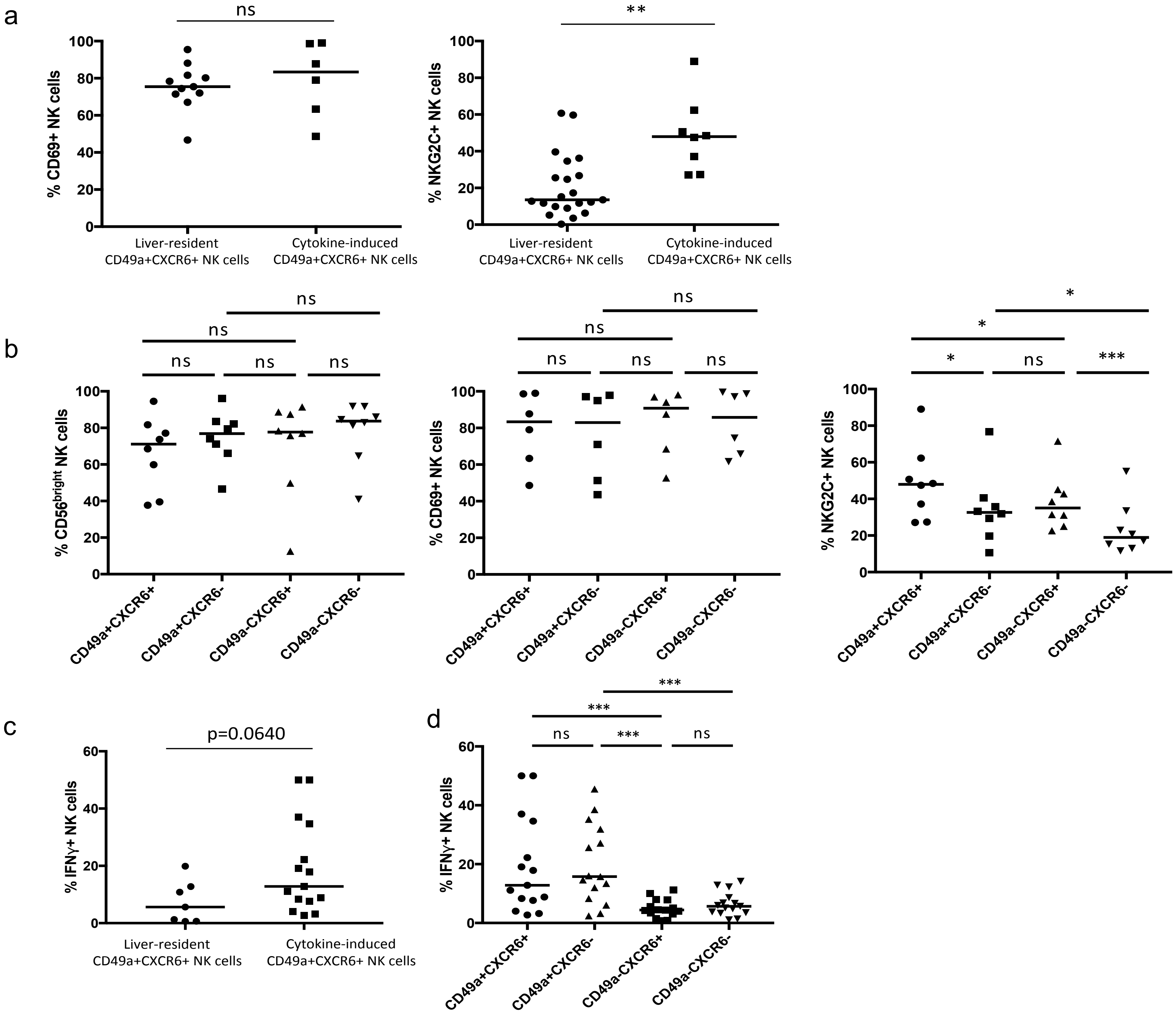
a
ns
% CD69+ NK cells
0
20
40
60
80
100
Liver-resident CD49a+CXCR6+ NK cells
Cytokine-induced CD49a+CXCR6+ NK cells
**
% NKG2C+ NK cells
0
20
40
60
80
100
Liver-resident CD49a+CXCR6+ NK cells
Cytokine-induced CD49a+CXCR6+ NK cells
b
ns
ns
ns
ns
ns
% CD56bright NK cells
0
20
40
60
80
100
CD49a+CXCR6+
CD49a+CXCR6-
CD49a-CXCR6+
CD49a-CXCR6-
ns
ns
ns
ns
ns
% CD69+ NK cells
0
20
40
60
80
100
CD49a+CXCR6+
CD49a+CXCR6-
CD49a-CXCR6+
CD49a-CXCR6-
*
*
*
ns
***
% NKG2C+ NK cells
0
20
40
60
80
100
CD49a+CXCR6+
CD49a+CXCR6-
CD49a-CXCR6+
CD49a-CXCR6-
c
p=0.0640
% IFNγ+ NK cells
0
20
40
60
Liver-resident CD49a+CXCR6+ NK cells
Cytokine-induced CD49a+CXCR6+ NK cells
d
***
***
ns
***
ns
% IFNγ+ NK cells
0
20
40
60
CD49a+CXCR6+
CD49a+CXCR6-
CD49a-CXCR6+
CD49a-CXCR6-

Supplementary Table 1. Patient demographic data

Demographic Details (n=52)	
Age, years (range)	65 (29-80)
Men, n (%)	32 (61.5)
Pre-operative chemotherapy, n (%)	29 (55.8)
Reason for resection, n (%)	
Metastases, colorectal	33 (63.5)
Metastases, other	8 (15.4)
Hepatocellular carcinoma	6 (11.5)
Cholangiocarcinoma	2 (3.8)
Gastrointestinal stromal tumour	1 (1.9)
Hepatic cyst	1 (1.9)
Lymphoma	1 (1.9)
Background liver histology, n (%)	
Normal	30 (57.7)
Mild steatosis	16 (30.8)
Moderate steatosis	3 (5.8)
Fibrosis	3 (5.8)
Clear resection margin	50 (96.2)

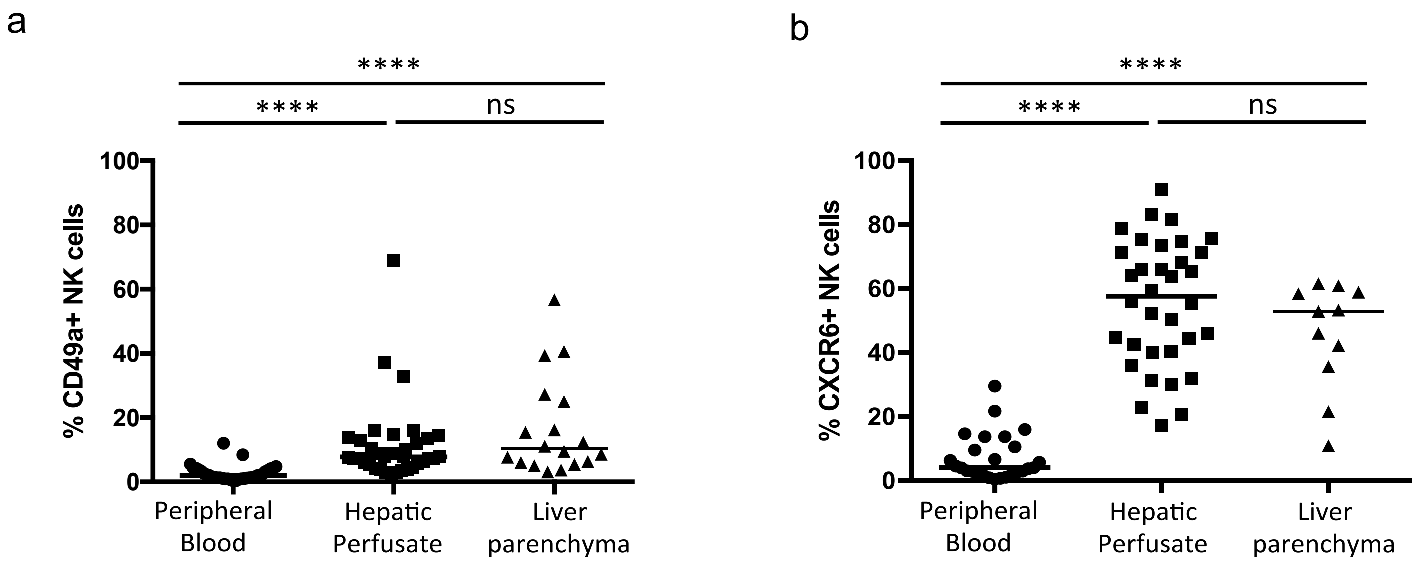

Supplementary Figure 1. a) A comparison of the frequency of CD49a+ NK cells within the peripheral blood, hepatic perfusate and liver parenchyma NK cell populations (paired and unpaired samples, n=35, n=35, n=18). Dot plots display individual values and median. (Mann Whitney U test). **b)** A comparison of the frequency of CD49a+ NK cells within the peripheral blood, hepatic perfusate and liver parenchyma NK cell populations (paired and unpaired samples, n=26, n=34, n=11). Dot plots display individual values and median. (Mann Whitney U test). $p<0.0001$****.

HEPATIC PERFUSATE

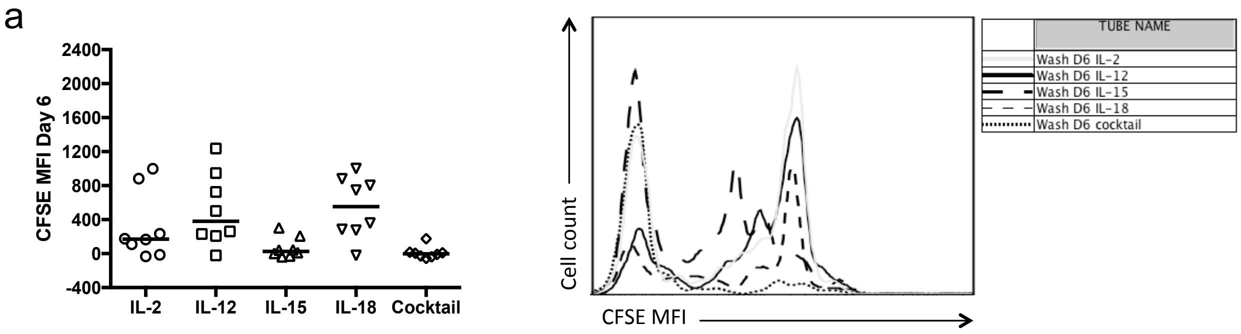

IL-2	IL-12	IL-15	IL-18	Cocktail
170	381.3	26.91	553.1	-2.58

PERIPHERAL BLOOD

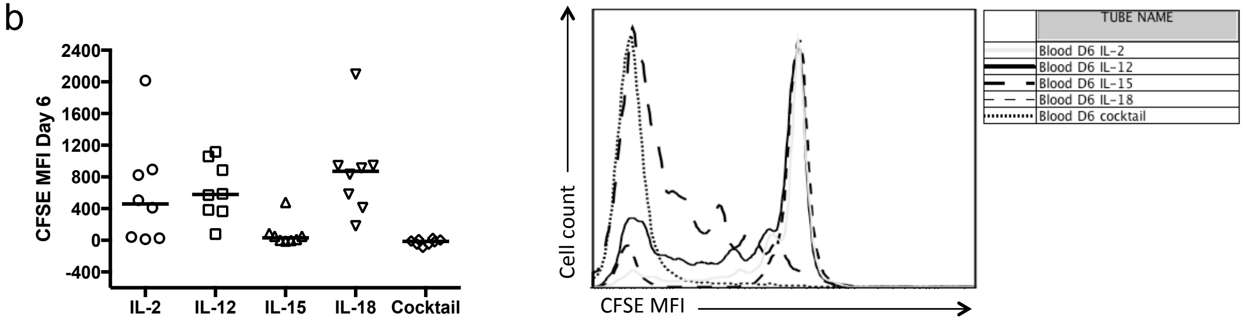

IL-2	IL-12	IL-15	IL-18	Cocktail
459.6	579.1	30.52	870.9	-13.11

Supplementary Figure 2. a) Day 6 CFSE MFI of hepatic NK cells following culture with IL-2, IL-12, IL-15, IL-18 and the cytokine cocktail. Median values displayed below**.** Dot plots display individual values and median. Representative flow cytometry histograms from one individual show CFSE expression at day 6 following culture with IL-2, IL-12, IL-15, IL-18 and the cytokine cocktail. **b)** Day 6 CFSE MFI of peripheral blood NK cells following culture with IL-2, IL-12, IL-15, IL-18 and the cytokine cocktail. Median values displayed below**.** Median values displayed below**.** Dot plots display individual values and median. Representative flow cytometry histograms from one individual show CFSE MFI at day 6 following culture with IL-2, IL-12, IL-15, IL-18 and the cytokine cocktail.

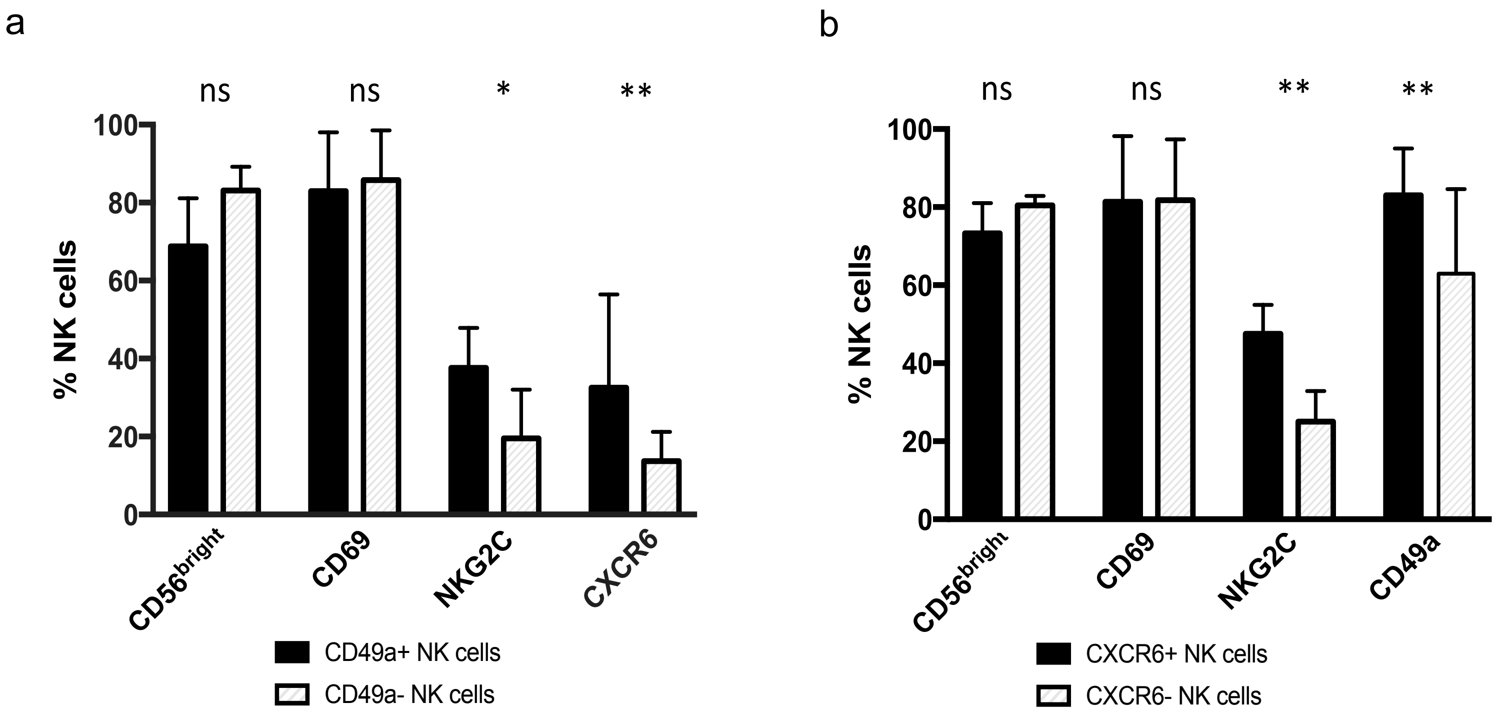

Supplementary Figure 3. **a)** A comparison of CD56^{bright}, CD69+, NKG2C+ and CXCR6+ NK cell frequencies found within CD49a+ and CD49a- NK subsets generated in the peripheral blood following 6 days of culture with IL-15 (n=9). Bar chart displays median and interquartile range. (Wilcoxon matched pairs test). **b)** A comparison of CD56^{bright}, CD69+, NKG2C+ and CD49a+ NK cell frequencies found within CXCR6+ and CXCR6- NK subsets generated in the peripheral blood following 6 days of culture with IL-15 (n=9). Bar chart displays median and interquartile range. (Wilcoxon matched pairs test). median. $p<0.05$*, $p<0.01$**.

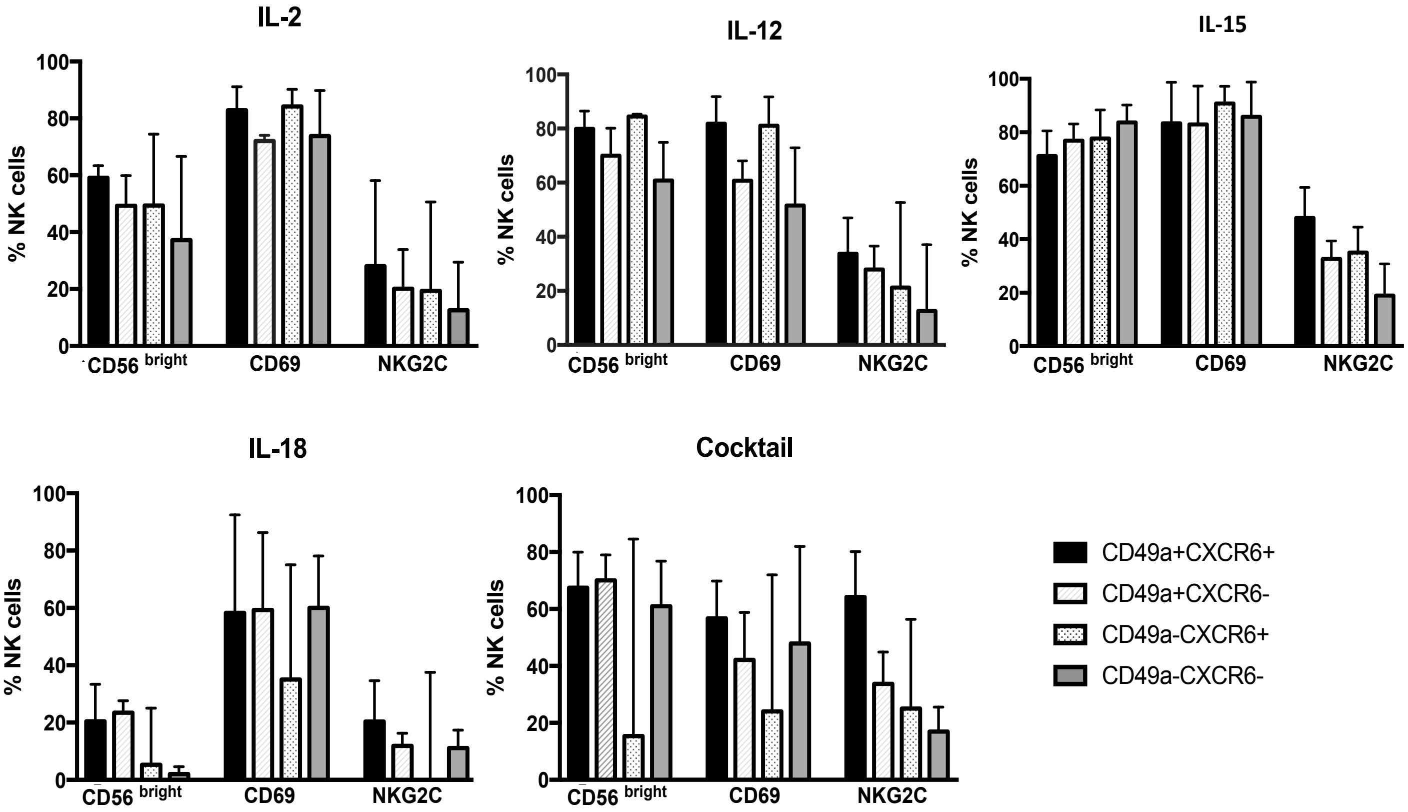

Supplementary Figure 4. A comparison of CD56^{bright}, CD69+ and NKG2C+ NK cell frequencies between CD49a+CXCR6+, CD49a+CXCR6-, CD49a-CXCR6+, CD49a-CXCR6- NK subsets generated in the peripheral blood following 6 days of culture with IL-2, IL-12, IL-15, IL-18 and a cocktail of all four cytokines (n=9). Bar chart displays median and interquartile range.